Article

Ex-Vivo Exposure on Biological Tissues in the 2-μm Spectral Range with an All-Fiber Continuous-Wave Holmium Laser

Mariya S. Kopyeva [1,2], **Serafima A. Filatova** [1,*], **Vladimir A. Kamynin** [1], **Anton I. Trikshev** [1], **Elizaveta I. Kozlikina** [1,3], **Vadim V. Astashov** [4], **Victor B. Loschenov** [1,3] **and Vladimir B. Tsvetkov** [1]

1 Prokhorov General Physics Institute of the Russian Academy of Sciences, 38 Vavilov St., 119991 Moscow, Russia; mashutka_kopyova@mail.ru (M.S.K.); kamyninva@gmail.com (V.A.K.); trikshevgpi@gmail.com (A.I.T.); kozlikina.ei@nsc.gpi.ru (E.I.K.); loschenov@nsc.gpi.ru (V.B.L.); tsvetkov@lsk.gpi.ru (V.B.T.)
2 Faculty of Science, Peoples Friendship University of Russia (RUDN University), 3 Ordzhonikidze St., 115419 Moscow, Russia
3 Institute for Physics and Engineering in Biomedicine, National Research Nuclear University MEPhI, 31 Kashirskoe Shosse, 115409 Moscow, Russia
4 Human Anatomy Department, Peoples Friendship University of Russia (RUDN University), 8 Miklukho-Maklaya St., 117198 Moscow, Russia; astashov_vv@pfur.ru
* Correspondence: filatova@kapella.gpi.ru

Abstract: We present the results on the interaction of an all-fiber Holmium-doped laser CW radiation at a wavelength of 2100 nm with soft tissues and compare it with the other results obtained by the most used solid-state laser systems. Ex-vivo single spot experiments were carried out on the porcine longissimus muscles by varying the laser impact parameters in a wide range (average output power 0.3, 0.5 and 1.1 W; exposure time 5, 30 and 60 s). Evaluation of the laser radiation exposure was carried out by the size of coagulation and ablation zones on the morphological study. Exposure to a power of 0.3 W (1.5–18 J of applied energy) caused only reversible changes in the tissues. The highest applied energy of 66 J for 1.1 W and a 60-s exposure resulted in a maximum ablation depth of approximately 1.2 mm, with an ablation efficiency of 35%. We have shown that it is not necessary to use high powers of CW radiation, such as 5–10 W in the solid-state systems to provide the destructive effects. Similar results can be achieved at lower powers using the simple all-fiber Holmium laser based on the standard single-mode fiber, which could provide higher power densities and be more convenient to manufacture and use. The obtained results may be valuable as an additional experimental point in the field of existing results, which in the future will allow one to create a simple optimal laser system for medical purposes.

1. Introduction

Currently, fiber laser sources are used in many technical and scientific fields, due to their numerous advantages in comparison with other laser systems (solid-state or gas); for example, a wide lasing wavelength range, a variety of commercially available components, the ability to obtain various operation modes (from continuous-wave to ultrashort pulses), stable output power, compactness and reliability of the design, as well as high beam quality [1,2]. Nowadays, lasing in the spectral range of 800–2210 nm [3,4] was demonstrated in lasers based on standard silica fibers doped with rare-earth ions. The maximum lasing wavelength in silica fibers is limited by 2200 nm, due to low luminescence quantum yield [5] and transparency losses in the short-wave infrared spectral range. Therefore, fibers with another glass matrix or structure [6] are used to operate in this range. Thus, the doping

of fibers with rare-earth ions, such as erbium (Er^{3+}), thulium (Tm^{3+}) and holmium (Ho^{3+}) makes it possible to obtain lasing in the spectral range of 1700–3000 nm, thereby expanding the application area of such systems [7].

The presence of water absorption peaks in the range of 2000 nm makes these laser systems prospective for medical applications [8], such as in urology, dermatology, cosmetic surgery and minimally-invasive surgery [9]. Much attention is paid to the issue of the laser radiation interaction with biological tissues, as it is an exciting topic that can influence socially significant issues. Therefore, numerous studies have been carried out since the 1980s–1990s, including the application of 2-μm CW radiation for tissue ablation. Thulium and holmium laser systems, mainly the solid-state Tm:YAG, Ho:YAG lasers or fiber lasers with bulk elements such as dichroic mirrors, are widely used for these studies [10–12]. Typically, these systems operate in a continuous-wave (CW) or in a high-energy pulsed regime with a pulse duration of 100–250 μs at a low repetition rate, and have the dependence of lasing characteristics on the active medium temperature, as well as thermal lensing in the laser crystals which could restrict the operating ranges [13]. This leads to the necessity of complex and expensive cooling systems, which increases the size and cost of the laser systems.

Due to the progress in the field of laser technology made since the 1990s, the designs of laser systems have also changed and improved. In accordance with this, laser technology for medicine must also be modernized, be more reliable, compact, easy to use, universal in terms of the used components and relatively cheap in cost and servicing. Fiber lasers could meet these points because of their numerous advantages listed above [14]. Furthermore, with the existing variety of pathologies, more individual treatment and an accurate selection of the optimal laser operating regimes are required, which ensures a decrease in injuries during operations. Additionally, the modern minimally-invasive surgery is impossible without endoscopic techniques, which gives an advantage to fiber lasers, which are fully compatible with existing surgical endoscopes. In addition, a decrease in source and service costs should be expected while using fiber systems. Therefore, research on the development and application of fiber laser systems for medical purposes is being actively carried out [15,16].

The result of laser radiation exposure on biological tissues depends on both biological material properties and laser radiation parameters: wavelength, power density, duration of exposure and the pulse repetition rate in the case of pulsed operation mode [17]. During laser radiation exposure on biological tissues, it is also necessary to take into account heat generation. During the CW radiation exposure, an increase in the temperature difference between the irradiated and surrounding tissue is observed. In this case, heat is transferred from the heated zone of biological tissue to the surrounding one, which can damage healthy tissue from overheating. During the pulsed radiation exposure, the dimensions of the heat-affected zone depend on the pulse duration and repetition rate, as well as the thermal diffusivity rate in biological tissue. With pulsed heating, the area of thermal damage is smaller due to the fact that the processes of light absorption and heat generation are fast and the heat diffusivity is slow [18,19].

The ablative mechanism observed during laser exposure to biological tissues corresponds well with the other authors' works [20–22]. Continuous exposure with both a Nd:YAG laser with a wavelength of 1064 nm [21] and a 2-micron Ho:YAG laser [20,22] shows explosive ablation and water vaporization in soft tissues. A detailed description of the fundamental issues of CW laser-tissue interaction was characterized by three distinct stages, as described previously in [23]. For a wavelength of 2100 nm, which corresponds to the Holmium laser generation wavelength, the water absorption coefficient is about 40 cm^{-1}. Thus, the radiation is absorbed in the surface tissues and penetrates to a depth of up to 1 mm. Due to heat diffusion, however, the laser damage zone can extend deeper into the irradiated tissue than the absorption length [24]. This allows a precise cut, and the heating of the near tissues provides sufficient hemostasis [22]. Meanwhile, Nd lasers

with an absorption coefficient of 2–10 cm^{-16} can only provide tissue coagulation, and CO_2 lasers frequently used in medicine exhibit cutting properties but no hemostasis [25].

Since the area of lasers application in medicine is quite wide, from therapeutic to surgical effects, it is very important to select the laser radiation parameters for each specific case, based on the required effect of exposure, leading to the reversible or irreversible damage of biological tissues [26]. For therapeutic effects, such as hyperthermia or the immune response activation (laser adjuvant), relatively low laser powers are needed, which would heat an area of biological tissue to a certain temperature without having a destructive effect on the healthy cells of biological tissue [27,28]. In the last decade, the surgical and neurosurgery applications of lasers for procedures with reduced collateral damage shows promising results [29,30]. Compact and robust fiber lasers with small-coating delivery fibers are also improving these results [31]. The use of laser radiation for these delicate procedures required exerting the effective precise and local destruction effect with minimal damage to healthy tissues [32]. The use of 2000 nm radiation leads to a decrease in the penetration depth, as well as to local tissue heating; this allows a precise effect on biological tissues. It is worth noting that 2000 nm radiation is safe for vision, which is an important advantage for such areas as atmospheric communications, location and medicine [33]. Since the absorption peak of water at a wavelength of about 1.94 µm, the use of a holmium-doped laser with radiation wavelengths slightly different from the absorption peak of water makes it possible to vary the penetration depth of the laser radiation [34,35].

In this work, we present the results on the all-fiber Ho-doped laser CW radiation interaction with soft tissue, and compare it with the other results obtained by the most used solid-state laser systems. A simple, robust and compact all-fiber Holmium system operated at a wavelength of 2100 nm. In the ex-vivo single-spot ablation experiments on the porcine longissimus muscle tissues, the depths and diameters of coagulation zones, ablation craters and thermal damage zones were evaluated after exposure to a wide range of applied energy (1.5–66 J). By varying the impact parameters (laser power, exposure time), we can demonstrate that this laser system can be adapted for thermal effects, tissue coagulation and tissue removal. It is worth noting that the review of such all-fiber Holmium laser systems for soft-tissue exposure has not been observed in the literature.

2. Materials and Methods

2.1. Ho-Doped Fiber Laser Operating in Continuous-Wave Mode

An all-fiber holmium laser operating in continuous-wave mode was used in our experiment. The experimental setup of the laser scheme is shown in Figure 1a. The Ho-doped fiber laser was pumped by Ytterbium-doped (Yb) fiber laser generating CW radiation with a maximum power of up to 13 W at a wavelength of 1125 nm. The Ho-doped silica fiber was used as an active medium of the laser. The fiber core diameter was 13 µm, holmium ions concentration in the active core was estimated as 2×10^{19} cm^{-3} and absorption coefficient at the pump wavelength (1125 nm) was about 5.2 dB/m. The optimized length of Ho-doped fiber in the laser cavity was 4.5 m. Fiber Bragg gratings (FBG) with high (99%) and low (20%) reflection coefficients at a wavelength of 2100 nm were used as the cavity mirrors. The use of standard silica-based fibers and components allowed us to implement an all-fiber robust and compact scheme with standard splices and quick emergency of any laser system problems. Therefore, the radiation is propagated and outcoupled through a single-mode fiber (core diameter 9–13 µm), in contrast to solid-state lasers, where the fiber with a diameter of more than 100 µm is often used for the radiation output. This approach will allow us to achieve higher power densities, and make this laser flexible and universal for experiments.
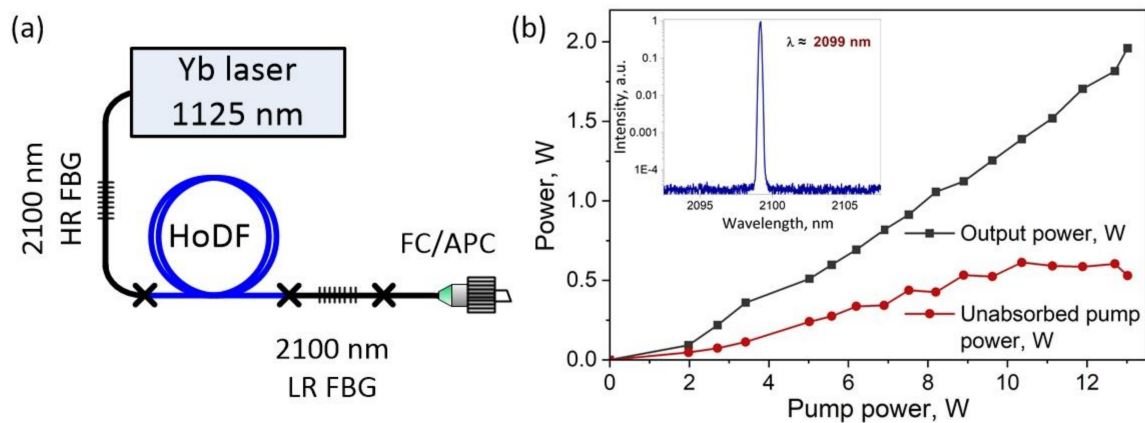
Figure 1. (**a**) Experimental setup of Ho-doped fiber laser operating in a CW mode; and (**b**) Dependence of the output power (black line and squares) and unabsorbed pump power (red line and dots) on the pump power; the lasing spectrum at $\lambda \approx 2099$ nm on the inset.

Figure 1b shows the output and unabsorbed pump power as a function of the input pump power. The inset in Figure 1b shows the lasing spectrum of a CW Ho-doped fiber laser measured by an optical spectrum analyzer, Yokogawa, with a spectral resolution of 0.1 nm. As can be seen, the lasing wavelength was about 2099 nm what corresponds to the FBGs reflection maxima and the linewidth measured at the half-maximum did not exceed 0.1 nm. A bandpass optical filter with a transmission in the spectral range of 1500–2500 nm was used to suppress the unabsorbed emission from the Yb-doped fiber laser. Therefore, the maximum output power of the Ho-doped fiber laser was about 2 W.

2.2. Ex-Vivo Tissue Preparation and Experimental Setup

The most commonly considered soft biological tissue types for investigation of laser-tissue interaction are liver, kidney, brain, skin, adipose and muscle tissues, as their optical properties are well known [8,36]. Based on the optical properties' studies of different tissues types (muscle, adipose, spinal cord and dura mater of the spinal cord) in the spectral range of 1.1–2.6 μm, presented in work [8], we can see that the absorption spectra of some tissues are relatively similar, and the main absorber is water. A significant difference in absorption bands is observed for adipose tissue. Thus, the porcine longissimus muscle tissue was used as an ex-vivo tissue model for our experiments of CW Ho-doped fiber laser radiation exposure. The muscle tissue was cooled to 4 °C immediately after the animal post mortem, and the experiments were performed within the next 48 h. The cooled tissue was sliced into small specimens of 5 mm thick, which were placed on a glass slide. The temperature of the specimens was increased to room temperature (22 °C) before the experiments, and the surface of specimens was sprayed with saline to prevent the tissue from dehydrating. The total number of prepared and investigated specimens was 27 pieces.

Schematic diagram of the experimental setup for laser radiation exposure on the muscle tissue is shown in Figure 2a. Laser radiation, delivered through a single-mode fiber with an angle polished connector (FC/APC), was focused through an optical objective (1) with 8 × 0.2 NA (LOMO) and positioned normal to the surface of the muscle tissue specimens (3). The losses on the optical objective did not exceed 15%. A glass slide with the specimen was placed on the movable platform (4) for the focal distance adjustment. We have used the optical bandpass filter (2) with a transmission in the spectral range of 1500–2500 nm to suppress the unabsorbed pumping emission at a wavelength of 1125 nm. Figure 2b shows the radiation distribution in the laser spot approximated by the Gaussian function. Thus, the laser beam diameter at the half maximum was estimated to be 40 μm.
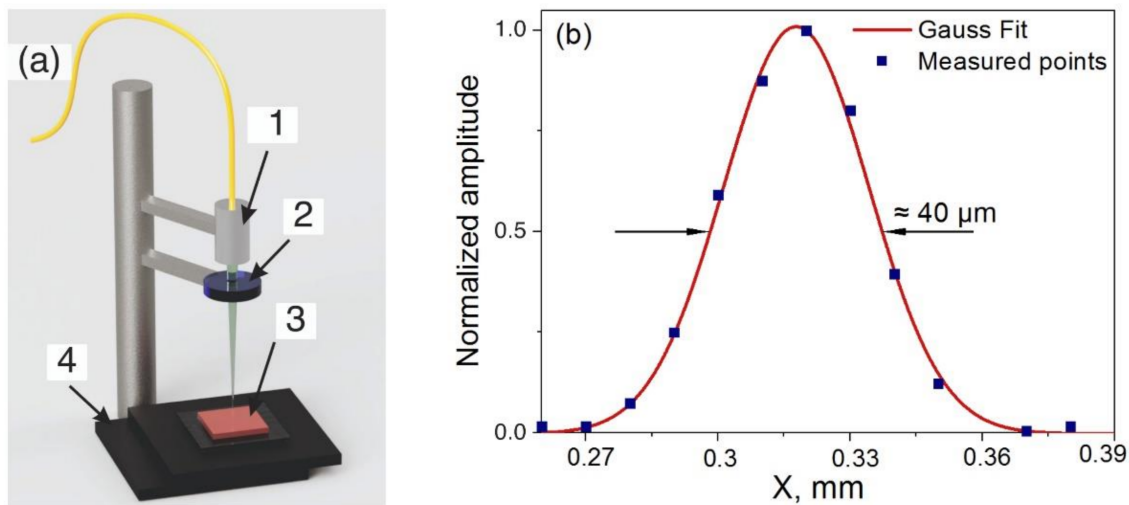
Figure 2. (**a**) Schematic diagram of the laser radiation exposure on the muscle tissue specimens: 1—an optical objective 8 × 0.2 NA (LOMO), 2—an optical bandpass filter, 3—a sample of the porcine longissimus muscle tissue, 4—a movable platform for the focal distance adjustment; (**b**) Power distribution of the Ho-doped fiber laser in the object plane of the lens (1).

The preliminary study of changes in the specimens' tissue surface was carried out immediately after exposure using an optical microscope (MBS-12), and was visually estimated. A more detailed and accurate morphological study of the coagulation, ablation, carbonization and heat-affected zones was carried out using the confocal laser scanning microscope Zeiss LSM 710 NLO with a tunable wavelength (800–1500 nm). Specimens were sectioned perpendicularly to the tissue surface using the Microtome cryostat Microm HM 540 (Thermo Fisher Scientific Microm International Gmbh, USA). Thus, we obtained cross-sectioned slices with 10 μm thickness at the site of laser radiation exposure. Then slices were stained with annexin 5/acridine orange-propidium iodide mixture to enable visualization of the thermal effects induced by laser radiation on tissues. Histological studies made it possible to determine the size of the coagulation zone, where the recovery of the affected cells by laser radiation is impossible.

2.3. Laser Parameters of Exposure

The preliminary study was carried out to determine the time and laser power for tissue exposure [37]. The exposure was carried out by CW radiation with a power of 0.25 W, 0.3 W and 0.83 W. The exposure time was varied from 1 to 60 s, and the size of the thermal damage zones was estimated using an optical microscope. The choice of these parameters was related to the time and laser power required for the appearance of noticeable changes (coagulation and carbonization) on the surface of the investigated tissue specimens. The obtained results are shown in Figure 3. As can be seen, the size of visible thermal damage zones on the tissue surface grows rapidly with increasing exposure time. After 30 s of exposure, the size of thermal damage zones does not change much. This effect can be explained by the evaporation of water from the tissue volume, which leads to a decrease in thermal conductivity to the surrounding tissue [38].
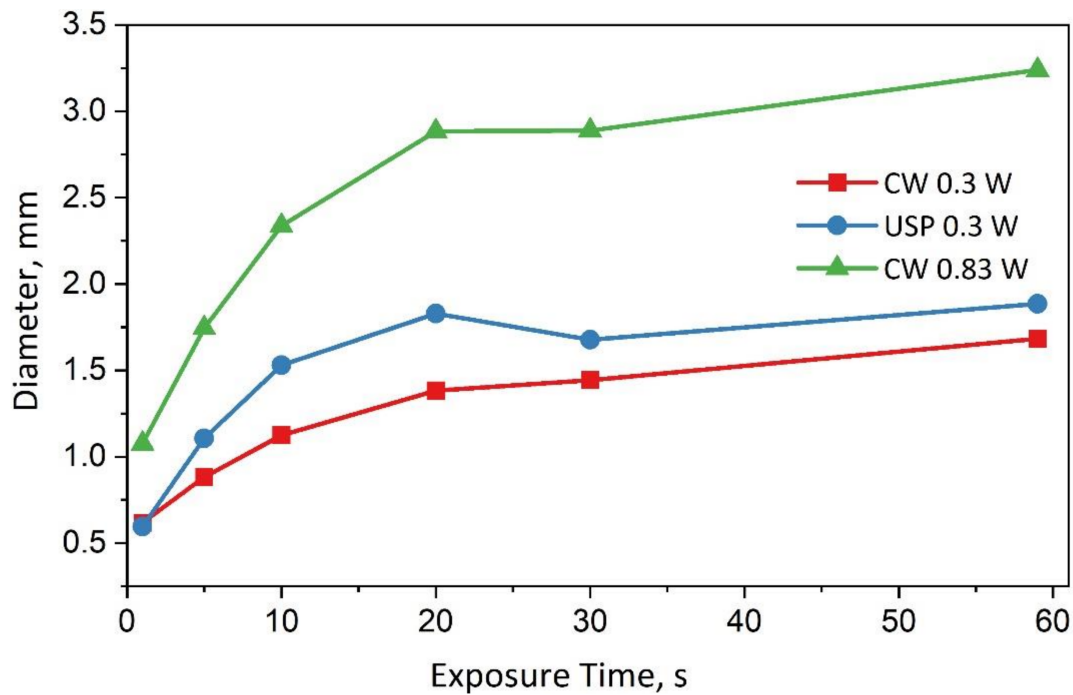
Figure 3. Dependence of the visible thermal damage diameter on the surface of porcine longissimus muscle tissue on the time of exposure by a different power of CW Ho-doped fiber laser: with 0.25 W (red line and squares), 0.3 W (blue line and circles) and 0.83 W (green line and triangles).

Based on the results obtained in [37] and the results presented in Figure 3, the following exposure times were chosen for the experiments with CW Ho-doped fiber laser radiation exposure: 5 s, 30 s and 60 s. The effect of CW laser radiation in a wide range of applied energy was achieved by choosing the laser power of 0.3 W, 0.5 W and 1.1 W, taking into account the losses on the optical objective. The value of applied energy (J), which was delivered to the tissue specimens, was estimated by multiplying the average power by the exposure time [11]. Table 1 shows the laser radiation parameters used in the single-spot experiments taking into account losses on the optical objective. The values of presented output power were measured after the bandpass filter.

Table 1. Parameters of CW Ho-doped fiber laser radiation used in the single-spot experiments.

Output Power, W	Power Density, W/cm^2	Exposure Time, s	Applied Energy, J
0.3	24×10^3	5	1.5
		30	9
		60	18
0.5	40×10^3	5	2.5
		30	15
		60	30
1.1	88×10^3	5	5.5
		30	33
		60	66

3. Results and Discussion

This research focused on the investigation of single-spot damage for different combinations of average output power and exposure time. It allowed us to understand the mechanism of ablative processes, as well as to clearly demonstrate qualitative changes in

the tissue during CW laser exposure and determine the values of power and time leading to reversible and irreversible effects in tissue.

Damage of the biological tissue surface can be divided into reversible and irreversible, which in turn are divided into different zones. These zones are schematically shown in Figure 4. Coagulation, carbonization and ablation zones can be attributed to irreversible damage, and the heat-affected zone is referred to as reversible damage. A preliminary visual estimation of the tissue surface damage size was carried out using the optical microscope, and a more accurate determination of the damage zones and their sizes was carried out using the confocal laser scanning microscope. Thus, the damage of the tissue surface was quantified by measuring the size of ablation, coagulation and heat-affected zones, as well as the carbonization tissue.
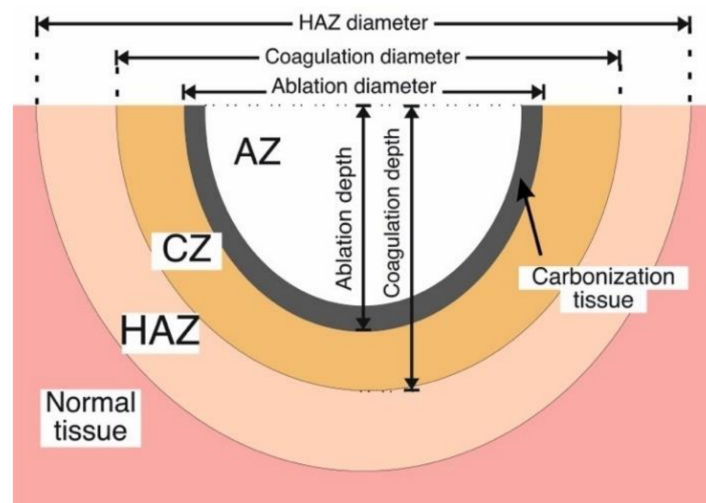

Figure 4. Schematic cross-section of the tissue showing definitions of tissue states: Normal tissue—unaffected tissue; heat-affected zone (HAZ)—reversible damage; irreversible damage includes coagulation zone (CZ), ablation zone (AZ) and carbonization tissue.

The effect of CW Ho-doped fiber laser radiation on longissimus muscle tissue can be seen in the microphotographs in Figure 5, which were obtained using the optical microscope (MBS-12). At the beginning of exposure, a zone of thermal damage is formed on the tissue surface, which can be identified by the changing of tissue color. The heat-affected zone (HAZ) is white, while the non-exposed tissue is light pink. The approximate boundaries of the HAZ area are marked by the red line. This zone grows over time from the center to the periphery. Further exposure leads to evaporation of water from the tissue and the appearance of cavitation effects, which are accompanied by audible clicks. At this point, the tissue is destructed and darkens around the emerging ablation crater. Additionally, the dehydrated tissue is darkened and turned into carbon, and we observe an ablation zone with a carbonization edge (marked with the yellow line).

Morphological studies made it possible to identify zones of tissue damage and describe them, as well as observe the propagation of laser energy deep into the tissue under study. Figure 6a shows a section of longissimus muscle tissue at the site of exposure by CW Ho-doped fiber laser with a power of 0.3 W for 30 s. As in the microphotograph (Figure 5a—30 s), only the heat-affected zone (HAZ) is observed here, which is characterized by the local edema without damaging the structure of the cells (myocytes). These changes are reversible, and may be accompanied by microcirculatory disturbances and temporary cellular dysfunction in response to local thermal effects of laser radiation. The boundaries of the HAZ zone in Figure 6b,c were not marked, as they went beyond the area of the microphotographs.
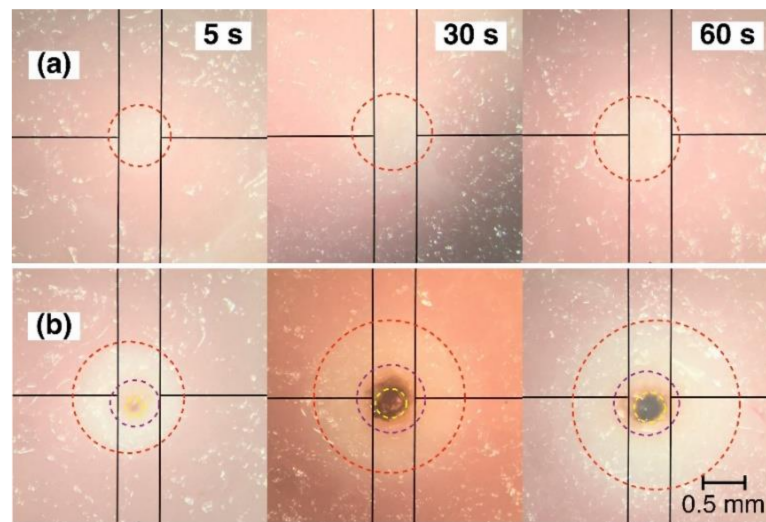
Figure 5. Microphotographs of the porcine longissimus muscle tissue surface after exposure by CW Ho-doped fiber laser with a power of (**a**) 0.3 W; and (**b**) 0.5 W for different times. The red line marks the total area of the heat-affected tissue; the purple line marks the total area of the coagulated tissue; and the yellow line marks an ablation zone with a carbonization edge.
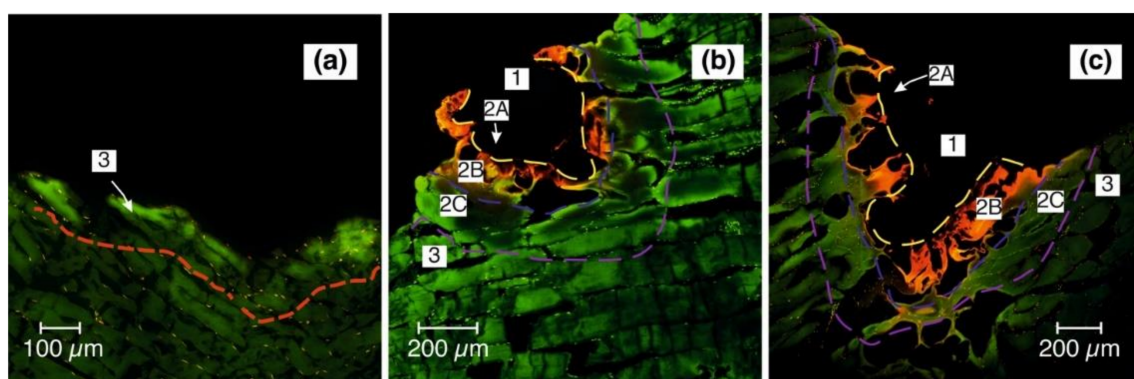

Figure 6. Longissimus muscle tissue after CW Ho-doped fiber laser exposure for 30 s with a power of (**a**) 0.3 W; and (**b**) 0.5 W; (**c**) 1.1 W. Notes: 1—Ablation zone (AZ), 2—Coagulation zone (CZ) with the elements of the coagulation crust and fragmentary charring, 3—heat-affected zone (HAZ).

Other results were observed after 30 s of exposure to CW Ho-doped fiber laser with an average output power of 0.5 W. A slight increase of output power – and as a consequence, of the applied energy – led to more serious damage (Figure 6b). In the ablation zone (AZ), the interstitial and intracellular fluid evaporates and the residue of dehydrated tissue burns off, resulting in the formation of an ablative crater. The coagulation zone (CZ) can be divided into three subzones: the burn border, the "spongy" and compact layers. The burn border or carbonization zone is formed due to the surface charring of the mineral components of myocytes (2A). The loose or "spongy" layer of coagulation necrosis (2B) is formed by necrotized myocytes with a vesicular altered cytoplasm. The compact layer of coagulation necrosis (2C) is myocyte dystrophy, and is formed due to the loss of water components. In blood vessels, there are coagulation of plasma, formed elements and vessel wall tissues with the formation of coagulated hyaline "thrombus" produced by laser exposure. We can then distinguish a heat-affected zone (3), which is characterized by local inflammatory swelling and is referred to as reversible damage. Figure 6c shows a histological slice for a specimen exposed to CW radiation with a power of 1.1 W for 30 s. The zones of ablation, coagulation and thermal effects are more visible in comparison with a power of 0.5 W, which is a consequence of the effect of higher applied energy to the biological tissue.

Figure 7 shows the diameters of the visible thermal damage zones (HAZ) for different values of applied energy of CW radiation. It is shown that an increase in the time and power of exposure leads to an increase in the HAZ diameter for all cases of CW laser radiation exposure. The minimum value of HAZ diameter of about 0.75 mm was obtained at the minimum laser power and time of exposure (0.3 W × 5 s = 1.5 J of applied energy). The maximum value of the HAZ diameter, of about 3.3 mm, was obtained after the CW laser radiation exposure with a power of 1.1 W for 60 s (66 J of applied energy). At the same time, there is no significant difference in the HAZ diameter after 1.1 W of CW laser radiation exposure for 30 and 60 s (33 and 66 J of applied energy). This may be due to the evaporation of water from the tissue volume during the exposure, which leads to a decrease in thermal conductivity to the surrounding tissue and to local accumulation of laser energy at the site of exposure.
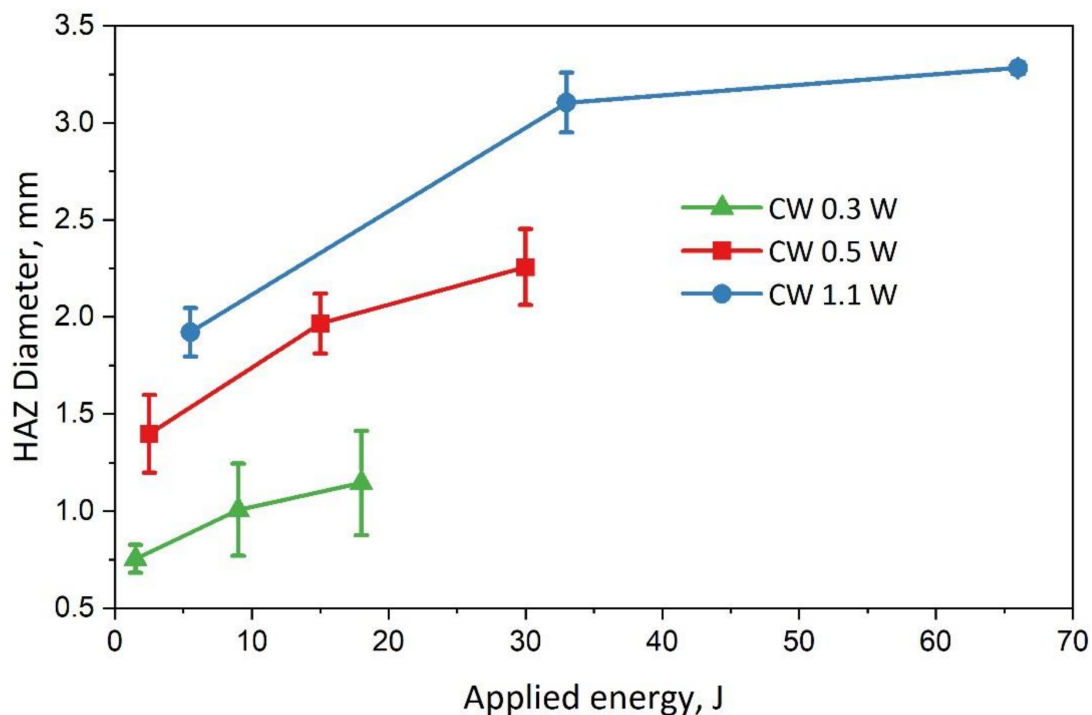

Figure 7. Dependency diagram of the heat-affected zone (HAZ) diameter on the applied energy of CW laser radiation for different times of exposure (5, 30 and 60 s) and laser power (0.3, 0.5 and 1.1 W).

For CW laser radiation with the lowest applied energy of 1.5 J (t = 5 s and power of 0.3 W), the formation of an ablation crater and tissue carbonization was not observed. Therefore, these values will not be presented in Figure 8, which shows the dependency diagrams of the depth and diameter of the coagulation and ablation zones on the applied energy of CW radiation with a power of 0.5 and 1.1 W. As can be seen in Figure 8, after CW radiation exposure with a power of 0.5 W for 5 s (2.5 J) and 1.1 W for 5 s (5.5 J), the ablation depth was about 0.2 mm. The dependence of the ablation depth on the exposure time was weak for CW laser radiation with an output power of 0.5 W. Meanwhile, for relatively high power (1.1 W), the depth of the ablation crater increased from 0.15 mm to 1.2 mm, with the exposure time increasing. The diameter of the ablation crater after radiation exposure with a power of 0.5 W was limited by 0.3 mm. For a power of 1.1 W, the ablation diameter increased from 0.2 mm up to 0.8 mm, alongside increasing the time of exposure. The maximum depth of the coagulation zones, obtained by CW radiation with a power of 0.5 W and 1.1 W, reached 0.6 mm and 2.1 mm, respectively. The maximum diameter of the coagulation zones reached 0.8 mm and 1.7 mm, for a CW power of 0.5 W and 1.1 W, respectively. The results show that the size of ablation and coagulation zones after exposure to relatively low-power laser radiation is weakly dependent on the applied

energy. Increasing the power up to 1.1 W – and as a consequence, the applied energy up to 66 J – leads to more serious destruction.
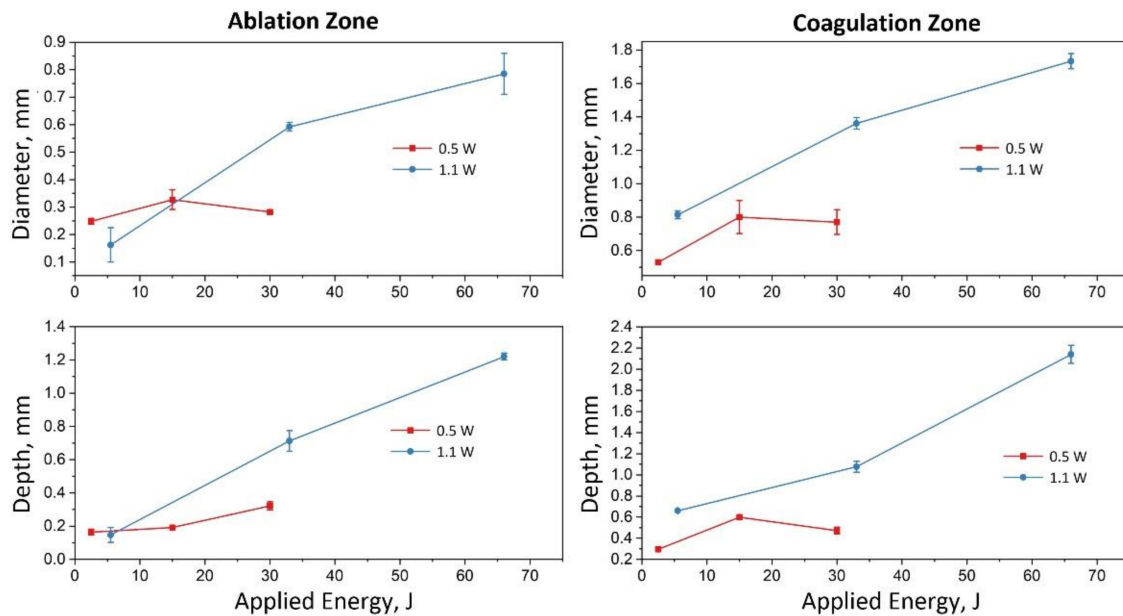

Figure 8. Dependency diagrams of the diameter and depth of ablation and coagulation zones on the applied energy of CW radiation for different times of exposure (5, 30 and 60 s) and laser power (0.5 and 1.1 W).

Quantitative estimation of the ablation processes observed during the CW laser radiation exposure with a power of 0.5 W and 1.1 W on biological tissues was carried out by calculating the ablation efficiency (*AE*) as a function of thermal damage [15,39]. We have measured thermally changed areas on histologically stained sections of specimens using the public domain software «ImageJ» (National Institutes of Health) [40]. The ratio of the ablation area (*AA*) to the total area of irreversible thermal damage, which includes the coagulation area (*CA*) and ablation area (*AA*), can be represented as:

$$AE, \% = \frac{AA}{AA + CA} \times 100 \qquad (1)$$

Figure 9 presents the obtained calculations in the graphs as a function of the applied energy of CW radiation. The ablation area (*AA*) obtained after exposure to a CW power of 0.5 W (red line with squares) and 1.1 W (blue line with circles) depended on the applied energy, and was increased up to 0.08 mm^2 and 1 mm^2, respectively. The coagulation area was also increased with the applied energy increasing (data not shown in the graph). Despite this, the ablation efficiency did not decrease and achieved a maximum of 35% for exposure to 66 J (power of 1.1 W and time 60 s), and 32% for 30 J (power of 0.5 W and time 60 s).

As noted earlier, most studies on the issue of 2-μm laser radiation interaction with soft tissues have used solid-state lasers (Tm:YAG, Ho:YAG, etc.) or fiber lasers with bulk elements [10,11,20,22,35]. Continuous-wave radiation from these lasers was delivered to the site of exposure using multimode fibers with a diameter of 200–600 μm, or by the lens sequence to focus laser radiation. The radiation power was usually in the range of 1–10 W. The tissues under ex-vivo exposure were porcine skin, kidney, liver and muscle, as well as chicken breast. Studies have shown that the diameter of thermal tissue destruction varies in the range of 400–750 μm, and the value of coagulation depth reaches 2 mm. These values are very close to what we obtained using an all-fiber Ho-doped laser system with lower powers.
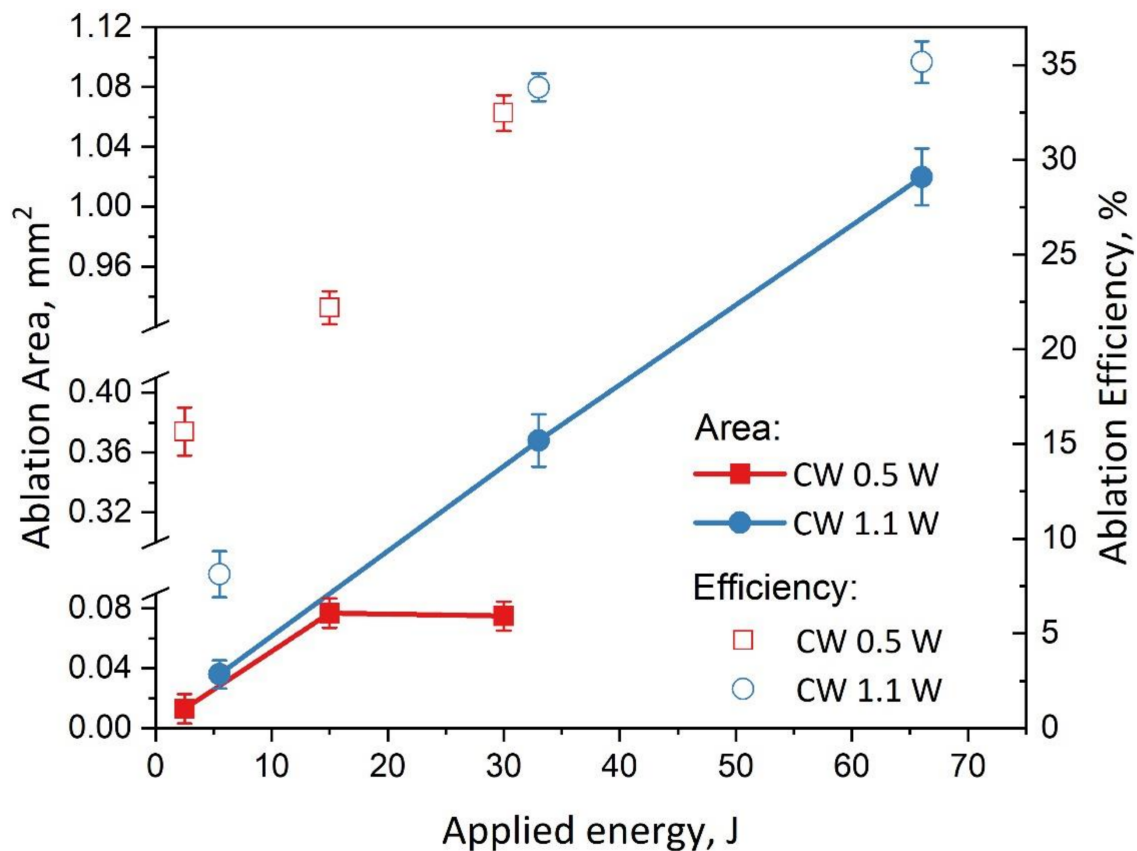
Figure 9. Ablation area and ablation efficiency as a function of applied energy of CW laser radiation for different times of exposure (5, 30 and 60 s) and laser power (0.5 and 1.1 W).

4. Conclusions

In this work, we have studied an all-fiber Ho-doped laser CW radiation interaction with soft tissue. A simple, robust and compact all-fiber system operated at a wavelength of 2100 nm. Ex-vivo single-spot experiments were carried out on the porcine longissimus muscles by varying the laser impact parameters (average output power and exposure time). The study of tissue destruction after laser radiation exposure was carried out by optical microscope, and the detailed morphological study was carried out by the study of histological slices on a confocal laser scanning microscope. As a result of lasers exposure to the tissue surface, characteristic laser wound zones were formed (ablation, coagulation and heat-affected zone).

We chose the output power levels of 0.3 W, 0.5 W and 1.1 W, and laser exposure intensity was regulated by the exposure time of 5 s, 30 s and 60 s. Thus, the lowest applied energy was 1.5 J for 0.3 W and 5 s of exposure. Experiments have shown that exposure to a power of 0.3 W for 5, 30 and 60 s (corresponding to 1.5, 9, 18 J of applied energy) leads only to the heat-affected zones formation. Only the local thermal damage with possible activation of the microvasculature links function was observed, which were reversible in character. The highest applied energy of 66 J for 1.1 W and a 60-s exposure to the tissue surface resulted in a rough tissue removal with a large affected area and carbonization edge, which is irreversible damage. The maximum achieved ablation depth and ablation efficiency were approximately 1.2 mm and 35%. Thus, increasing the laser energy to the tissue leads to increased areas of irreversible damage, coagulation and carbonization formatting. Very often in surgical practice, the carbonization of tissue is undesirable as the carbonized tissue is subjected to the extension of the healing period, and as a consequence, the higher risk of infection [13]. Based on the above and obtained results for the CW

Ho-doped fiber laser, we believe that the therapeutic effect is permissible at exposure with a power of 0.3 W within 60 s or less. For surgical effect with minimal carbonization edge formation, the exposure with a power of 0.5 W within 60 s may be enough. The higher powers can be used to obtain the ablative effects in a shorter exposure time. Thus, by varying two parameters, such as output power and time of exposure, it is possible to achieve the required effect from non-destructive tissue heating to tissue destruction.

On the other hand, for the application of 2-micron lasers to affect such sensitive organs as the spinal cord or the brain, possibly large ablation values are not required. In this case, the laser radiation effect must be as point and local as possible, and does not propagate deep into the tissue, so as not to damage vital tissues and blood vessels, as well as nerve endings.

Thus, we have shown that it is not necessary to use high powers of CW radiation, such as 5–10 W, to provide the destructive effects. Similar results can be achieved at lower powers using the simple all-fiber Holmium laser based on the standard single-mode fiber, which could provide higher power densities and be more convenient to manufacture and use. It is worth noting that the review of such all-fiber Holmium laser systems for soft-tissue exposure has not been observed in the literature. The obtained results may be valuable, as in the general power range and existing results, an additional experimental point appears, which in future will allow one to create simple optimal laser systems for medical purposes. The obtained data will be reference values for subsequent comparison with the results of exposure to ultrashort pulses in the 2-μm spectral range, as well as a starting point for *in-vivo* experiments.

Author Contributions: Conceptualization, V.B.T.; methodology, M.S.K., S.A.F., V.A.K., A.I.T. and E.I.K.; investigation, M.S.K., S.A.F., V.A.K. and E.I.K.; data analysis, M.S.K., V.V.A., S.A.F. and V.B.T.; writing—original draft preparation and editing, M.S.K., S.A.F., V.B.T., V.A.K., V.V.A. and V.B.L.; visualization, M.S.K. and S.A.F.; supervision, S.A.F.; and project administration, V.B.T. All authors have read and agreed to the published version of the manuscript.

Institutional Review Board Statement: Not applicable.

Informed Consent Statement: Informed consent was obtained from all subjects involved in the study.

Data Availability Statement: The data supporting the findings of this study are available within the article.

Conflicts of Interest: The authors declare no conflict of interest.

References

1. Shi, W.; Fang, Q.; Zhu, X.; Norwood, R.A.; Peyghambarian, N. Fiber lasers and their applications. *Appl. Opt.* **2014**, *53*, 6554–6568. [CrossRef]
2. Gursel, A.T. Fiber lasers and their medical applications. In *Optical Amplifiers—A Few Different Dimensions*; Intech Open: London, UK, 2018. [CrossRef]
3. Holmen, L.G.; Shardlow, P.C.; Barua, P.; Sahu, J.K.; Simakov, N.; Hemming, A.; Clarkson, W.A. Tunable holmium-doped fiber laser with multiwatt operation from 2025 nm to 2200 nm. *Opt. Lett.* **2019**, *44*, 4131–4134. [CrossRef] [PubMed]
4. Antipov, S.O.; Kamynin, V.A.; Medvedkov, O.I.; Marakulin, A.V.; Minashina, L.A.; Kurkov, A.S.; Baranikov, A.V. Holmium fibre laser emitting at 2.21 μm. *Quantum Electron.* **2013**, *43*, 603. [CrossRef]
5. Alekseev, N.E.; Izyneev, A.A.; Kravchenko, V.B.; Rudnitskii, Y.P. Influence of the concentration quenching and of water on the energy characteristics of neodymium-activated glasses. *Sov. J. Quantum Electron.* **1975**, *4*, 1111. [CrossRef]
6. Falconi, M.C.; Laneve, D.; Prudenzano, F. Advances in mid-IR fiber lasers: Tellurite, fluoride and chalcogenide. *Fibers* **2017**, *5*, 23. [CrossRef]
7. Ma, J.; Qin, Z.; Xie, G.; Qian, L.; Tang, D. Review of mid-infrared mode-locked laser sources in the 2.0 μm–3.5 μm spectral region. *Appl. Phys. Rev.* **2019**, *6*, 021317. [CrossRef]
8. Filatova, S.A.; Shcherbakov, I.A.; Tsvetkov, V.B. Optical properties of animal tissues in the wavelength range from 350 to 2600 nm. *J. Biomed. Opt.* **2017**, *22*, 035009. [CrossRef]

9. Serebryakov, V.A.; Boĭko, É.V.; Petrishchev, N.N.; Yan, A.V. Medical applications of mid-IR lasers. Problems and prospects. *J. Opt. Technol.* **2010**, *77*, 6–17. [CrossRef]

10. Huusmann, S.; Wolters, M.; Kramer, M.W.; Bach, T.; Teichmann, H.O.; Eing, A.; Herrmann, T.R. Tissue damage by laser radiation: An in vitro comparison between Tm: YAG and Ho: YAG laser on a porcine kidney model. *Springerplus* **2016**, *5*, 1–8. [CrossRef] [PubMed]

11. Antipov, O.L.; Zakharov, N.G.; Fedorov, M.; Shakhova, N.M.; Prodanets, N.N.; Snopova, L.B.; Sharkov, V.V.; Sroka, R. Cutting effects induced by 2 μm laser radiation of cw Tm: YLF and cw and Q-switched Ho: YAG lasers on ex-vivo tissue. *Med. Laser Appl.* **2011**, *26*, 67–75. [CrossRef]

12. Serebryakov, V.S.; Boĭko, É.V.; Kalintsev, A.G.; Kornev, A.F.; Narivonchik, A.S.; Pavlova, A.L. Mid-IR laser for high-precision surgery. *J. Opt. Technol.* **2015**, *82*, 781–788. [CrossRef]

13. Jones, P.S. Development and characterisation of holmium and erbium lasers for the ablation of biological tissue. Ph.D. Thesis, University of London, University College London, London, UK, 1993.

14. Blackmon, R.L.; Fried, N.M.; Irby, P.B. Comparison of holmium: YAG and thulium fiber laser lithotripsy: Ablation thresholds, ablation rates, and retropulsion effects. *J. Biomed. Opt.* **2011**, *16*, 071403. [CrossRef] [PubMed]

15. Alagha, H.Z.; Gülsoy, M. Photothermal ablation of liver tissue with 1940-nm thulium fiber laser: An ex vivo study on lamb liver. *J. Biomed. Opt.* **2016**, *21*, 015007. [CrossRef] [PubMed]

16. Tunc, B.; Gulsoy, M. Tm: Fiber laser ablation with real-time temperature monitoring for minimizing collateral thermal damage: Ex vivo dosimetry for ovine brain. *Lasers Surg. Med.* **2013**, *45*, 48–56. [CrossRef]

17. Sliney, D.H.; Trokel, S.L. *Medical Lasers and Their Safe Use*, 1st ed.; Springer Science & Business Media: New York, NY, USA, 1993; p. 230. [CrossRef]

18. Vogel, A.; Venugopalan, V. Mechanisms of pulsed laser ablation of biological tissues. *Chem. Rev.* **2003**, *103*, 577–644. [CrossRef]

19. Hoy, C.L.; Ferhanoglu, O.; Yildirim, M.; Kim, K.H.; Karajanagi, S.S.; Chan, K.M.C.; Kobler, J.B.; Zeitels, S.M.; Ben-Yakar, A. Clinical ultrafast laser surgery: Recent advances and future directions. *IEEE J. Sel. Top. Quantum Electron.* **2013**, *20*, 242–255. [CrossRef]

20. Pierce, M.C.; Jackson, S.D.; Dickinson, M.R.; King, T.A. Laser-tissue interaction with a high-power 2-μm fiber laser: Preliminary studies with soft tissue. *Lasers Surg. Med.* **1999**, *25*, 407–413. [CrossRef]

21. Verdaasdonk, R.M.; Borst, C.; Van Gemert, M.J.C. Explosive onset of continuous wave laser tissue ablation. *Phys. Med. Biol.* **1990**, *35*, 1129–1144. [CrossRef] [PubMed]

22. Domankevitz, Y.; McMillan, K.; Nishioka, N.S. Characterization of tissue ablation with a continuous wave holmium laser. *Lasers Surg. Med.* **1996**, *19*, 97–102. [CrossRef]

23. LeCarpentier, G.L.; Motamedi, M.; McMath, L.P.; Rastegar, S.; Welch, A.J. Continuous wave laser ablation of tissue: Analysis of thermal and mechanical events. *IEEE Trans. Biomed. Eng.* **1993**, *40*, 188–200. [CrossRef]

24. Herrmann, T.R.; Liatsikos, E.N.; Nagele, U.; Traxer, O.; Merseburger, A.S. EAU Guidelines Panel on Lasers. *Eur. Urol.* **2012**, *61*, 783–795. [CrossRef]

25. Wollin, T.A.; Denstedt, J.D. The Holmium Laser in Urology. *J. Clin. Laser Med. Surg.* **1998**, *16*, 13–20. [CrossRef]

26. Wieneke, S.; Gerhard, C. *Lasers in Medical Diagnosis and Therapy*; IOP Publishing: Bristol, UK, 2018. [CrossRef]

27. Skandalakis, G.P.; Rivera, D.R.; Rizea, C.D.; Bouras, A.; Jesu Raj, J.G.; Bozec, D.; Hadjipanayis, C.G. Hyperthermia treatment advances for brain tumors. *Int. J. Hyperth.* **2020**, *37*, 3–19. [CrossRef]

28. Kashiwagi, S. Laser adjuvant for vaccination. *FASEB J.* **2020**, *34*, 3485–3500. [CrossRef]

29. Belykh, E.; Yagmurlu, K.; Martirosyan, N.L.; Lei, T.; Izadyyazdanabadi, M.; Malik, K.M.; Byvaltsev, V.A.; Nakaji, P.; Preul, M.C. Laser application in neurosurgery. *Surg. Neurol. Int.* **2017**, *8*, 274. [CrossRef]

30. Pyo, H.; Kim, H.; Kang, H.W. Evaluations on laser ablation of ex vivo porcine stomach tissue for development of Ho: YAG-assisted endoscopic submucosal dissection (ESD). *Lasers Med. Sci.* **2021**, *36*, 1437–1444. [CrossRef]

31. Huang, Y.; Jivraj, J.; Zhou, J.; Ramjist, J.; Wong, R.; Gu, X.; Yang, V.X. Pulsed and CW adjustable 1942 nm single-mode all-fiber Tm-doped fiber laser system for surgical laser soft tissue ablation applications. *Opt. Express* **2016**, *24*, 16674–16686. [CrossRef]

32. Tunc, B.; Gulsoy, M. Stereotaxic laser brain surgery with 1940-nm Tm: Fiber laser: An in vivo study. *Lasers Surg. Med.* **2019**, *51*, 643–652. [CrossRef]

33. Scholle, K.; Lamrini, S.; Koopmann, P.; Fuhrberg, P. 2 μm laser sources and their possible applications. In *Frontiers in Guidedwave Optics and Optoelectronics*; Bishnu, P., Ed.; IntechOpen: Rijeka, Croatia, 2010; p. 674. [CrossRef]

34. Fried, N.M.; Murray, K.E. High-power thulium fiber laser ablation of urinary tissues at 1.94 μm. *J. Endourol.* **2005**, *19*, 25–31. [CrossRef]

35. Khoder, W.; Zilinberg, K.; Waidelich, R.M.; Stief, C.G.; Becker, A.J.; Pangratz, T.; Henning, G.; Sroka, R. Ex vivo comparison of the tissue effects of six laser wavelengths for potential use in laser supported partial nephrectomy. *J. Biomed. Opt.* **2012**, *17*, 068005. [CrossRef]

36. Bashkatov, A.N.; Genina, E.A.; Tuchin, V.V. Optical properties of skin, subcutaneous, and muscle tissues: A review. *J. Innov. Opt. Health Sci.* **2011**, *4*, 9–38. [CrossRef]

37. Kopyeva, M.S.; Filatova, S.A.; Kamynin, V.A.; Chekhlova, T.K.; Tsvetkov, V.B. Comparison of Continuous Wave and Ultrashort Pulsed Holmium-doped Fiber Lasers Exposure on Ex-vivo Tissue. In Proceedings of the 2021 Conference on Lasers and Electro-Optics Europe & European Quantum Electronics Conference (CLEO/Europe-EQEC), Munich, Germany, 20–24 June 2021; IEEE: New York, NY, USA, 2021; p. 1. [CrossRef]

38. El-Sherif, A.F.; King, T.A. Soft and hard tissue ablation with short-pulse high peak power and continuous thulium-silica fibre lasers. *Lasers Med. Sci.* **2003**, *18*, 139–147. [CrossRef] [PubMed]
39. Tunc, B.; Gulsoy, M. The Comparison of Thermal Effects of a 1940-nm Tm: Fiber Laser and 980-nm Diode Laser on Cortical Tissue: Stereotaxic Laser Brain Surgery. *Lasers Surg. Med.* **2020**, *52*, 235–246. [CrossRef] [PubMed]
40. Image Processing and Analysis in Java. Available online: https://imagej.nih.gov/ij/index.html (accessed on 29 October 2021).